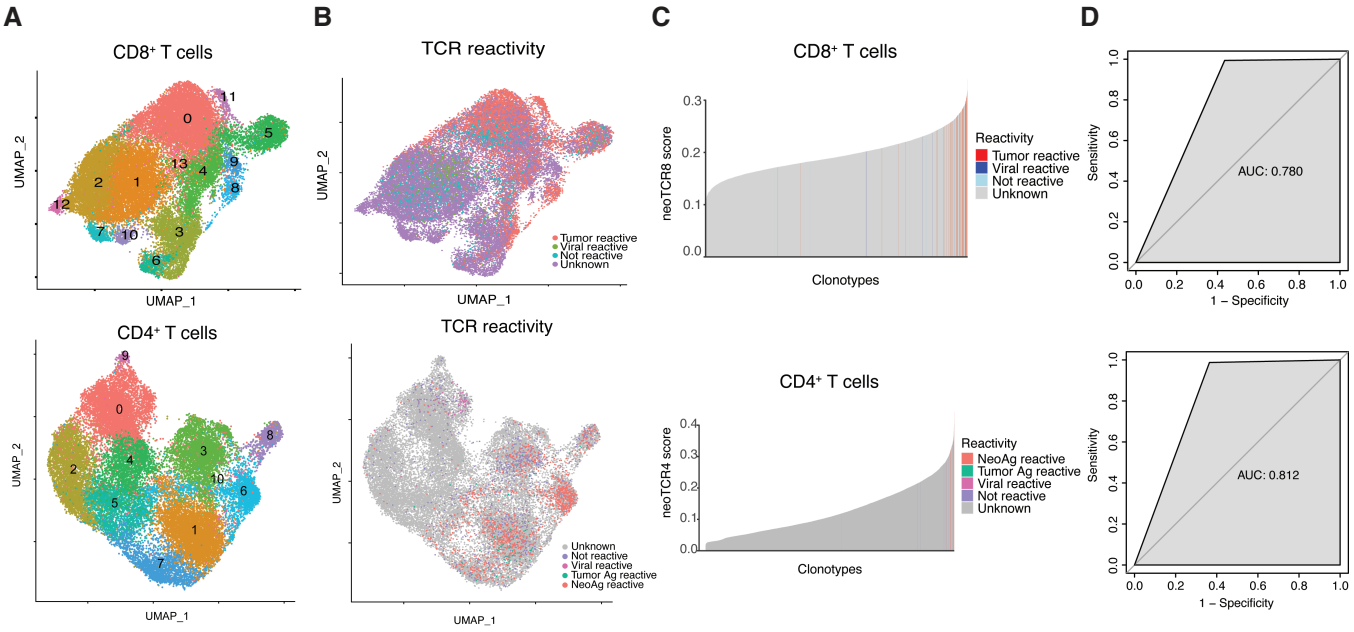

Figure S1: Transcriptional prediction of tumor antigen reactivity in functionally-validated tumor-infiltration CD8⁺ (top row) and CD4⁺ (bottom row) T cell reference dataset from patients with melanoma (*5, 6*). A-B) UMAP dimensionality reduction plots of tumor-infiltrating T cells labeled with transcriptional clusters (A) or experimentally-validated antigen reactivity. C) Histogram of neoTCR module scores for each T cell clonotype, colored by antigen reactivity. D) Receiving operating characteristic curve of predicted reactivity based on neoTCR labeling.

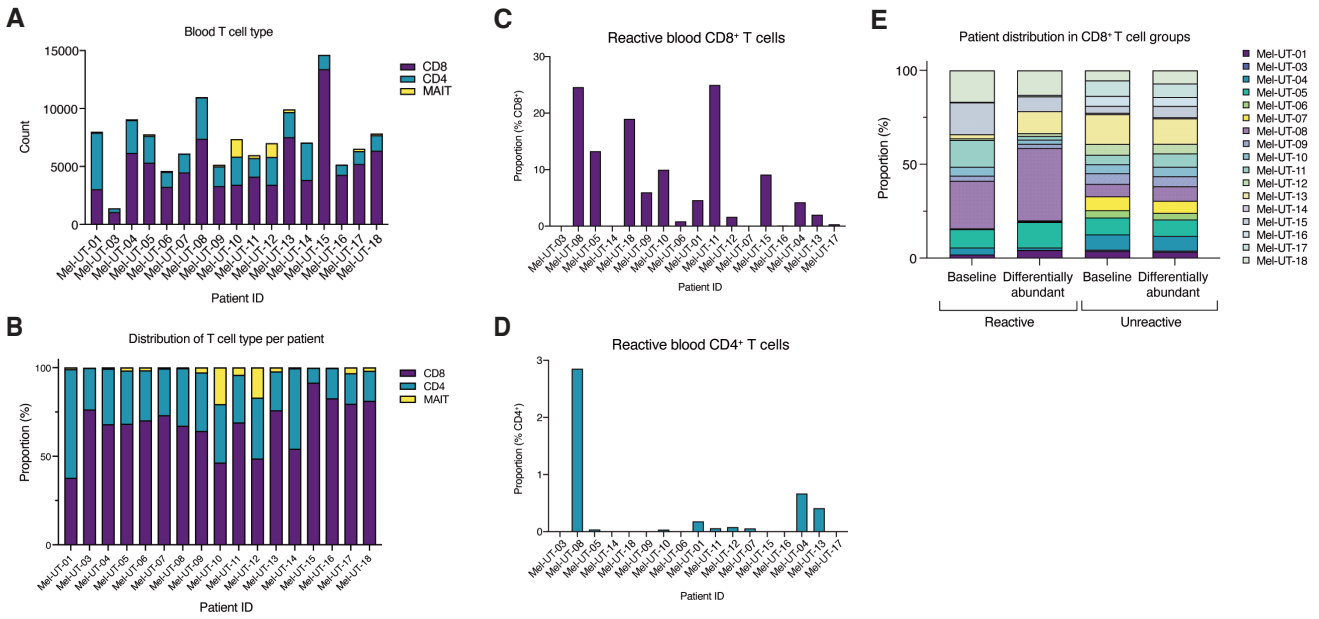

Figure S2: T cell distributions by patient in single-cell sequencing cohort. A-B) CD8⁺, CD4⁺, and MAIT T cells by cell number (A) or proportion (B). C-D) The proportion of predicted-reactive blood CD8⁺ (C) or CD4⁺ (D) T cells by patient. E) The proportion of patients in all predicted-reactivity (”Baseline”) or differentially abundant groups.

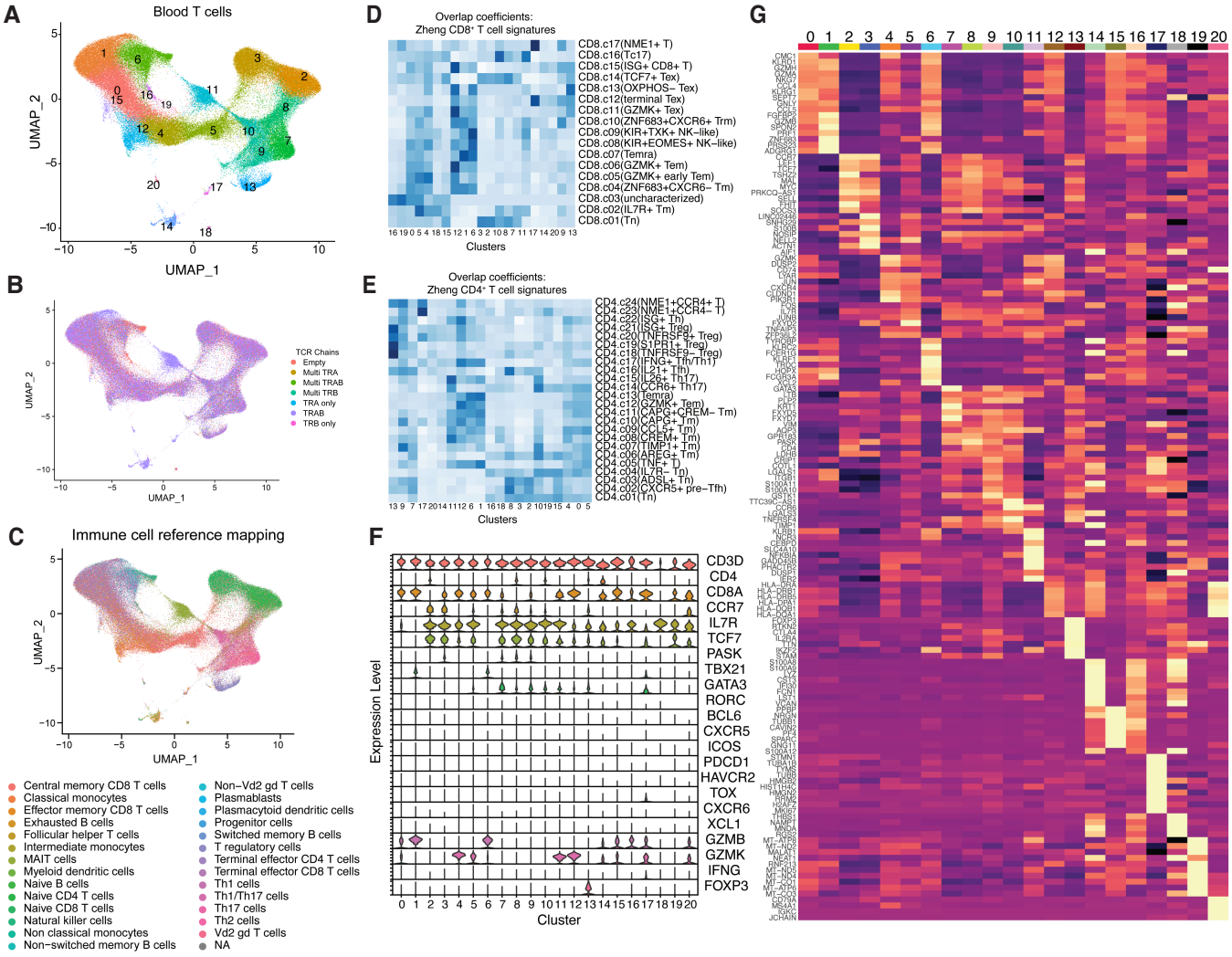

Figure S3: Phenotyping circulating T cells from patients with melanoma using single-cell RNA and paired T cell receptor (TCR) sequencing. A-C) UMAP dimensionality reduction plots of T cells in the blood labeled with transcriptional clusters (A), TCR chains (B), or automated label assignments using the SingleR package (C). Cell labels were based on bulk RNA sequencing signatures from sorted human peripheral blood mononuclear cells (*41*). D-E) Heatmap representation of overalap scores calculated against single-cell RNA sequencing atlases of CD8⁺ T cells (D) or CD4⁺ T cells (E) from patients with cancer (*40*). F) Violin plots of canonical T cell lineage genes in each transcriptional cluster. F) Heatmap of the top 10 differentially expressed genes across each transcriptional cluster.

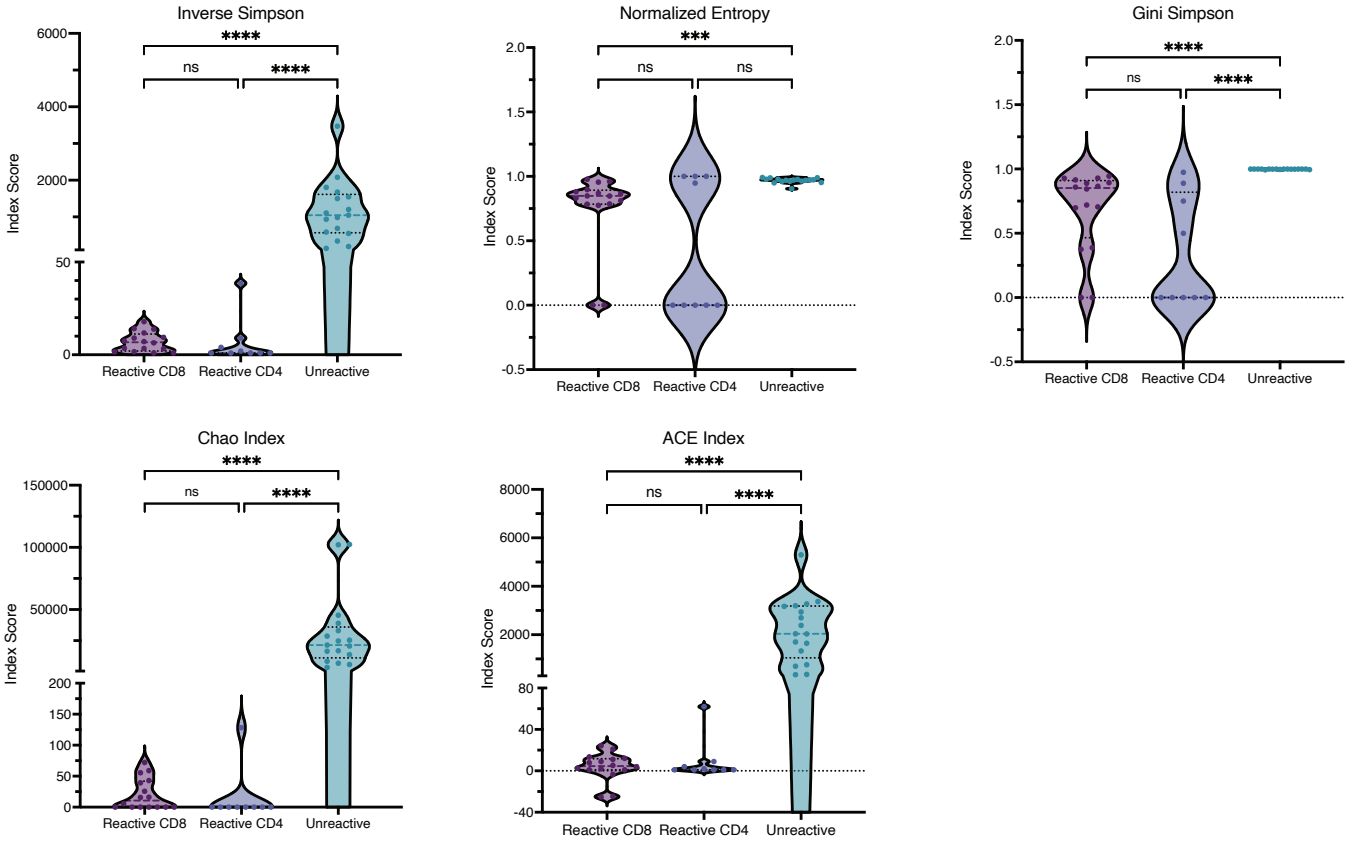

Figure S4: T cell receptor repertoire diversity in predicted-reactive CD8⁺ (Reactive CD8), predicted-reactive CD4⁺ (Reactive CD4), and unreactive (Unreactive) circulating T cells from patients with melanoma. Between group differences were determined with Kruskal–Wallis one-way analysis of variance testing ($p < 0.05$, **** $p < 0.0001$).

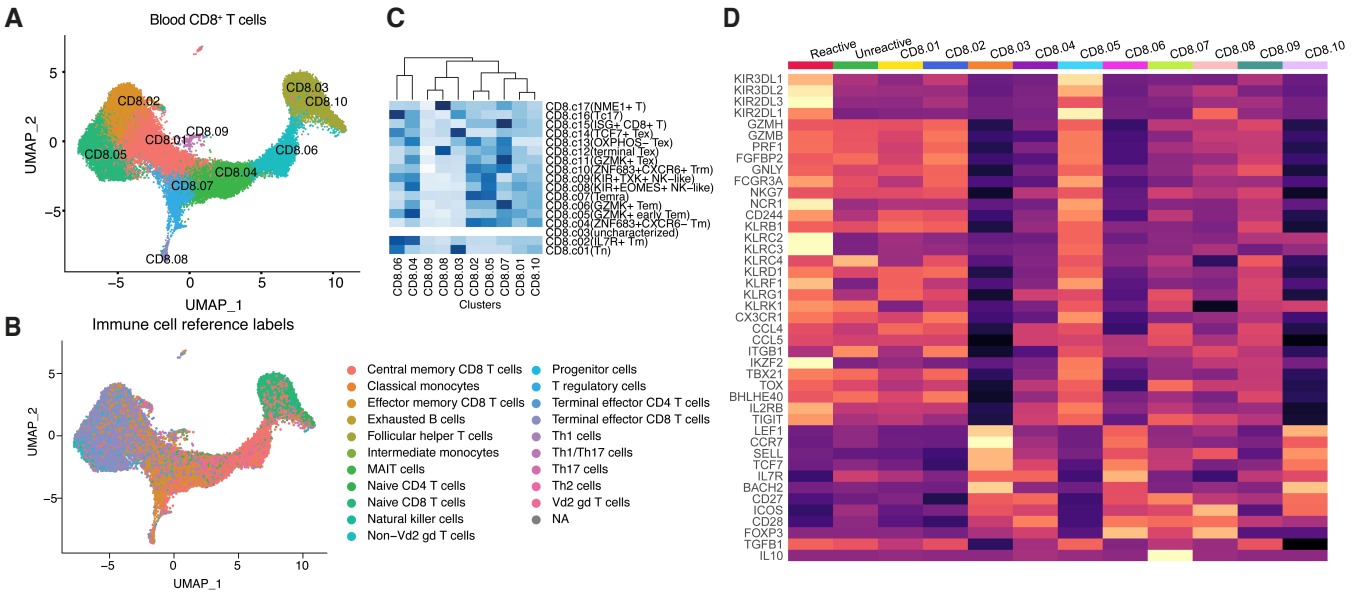

Figure S5: CD8⁺ T cells phenotyping using single-cell RNA sequencing. A) UMAP dimensionality reduction plot of blood-based CD8⁺ T cells labeled with transcriptional clusters or B) automated label assignments using the SingleR package. Cell labels were based on bulk RNA sequencing signatures from sorted human peripheral blood mononuclear cells (*41*). C) Heatmap representation of overalap scores calculated against a single-cell RNA sequencing CD8⁺ T cell atlas from patients with cancer (*40*). D) Heatmap of the expression of hallmark genes from human KIR⁺CD8⁺ T cells across differentially abundant predicted-reactive (Reactive), differentially abundant predicted-unreactive (Unreactive), and all other CD8⁺ T cell transcriptional clusters.

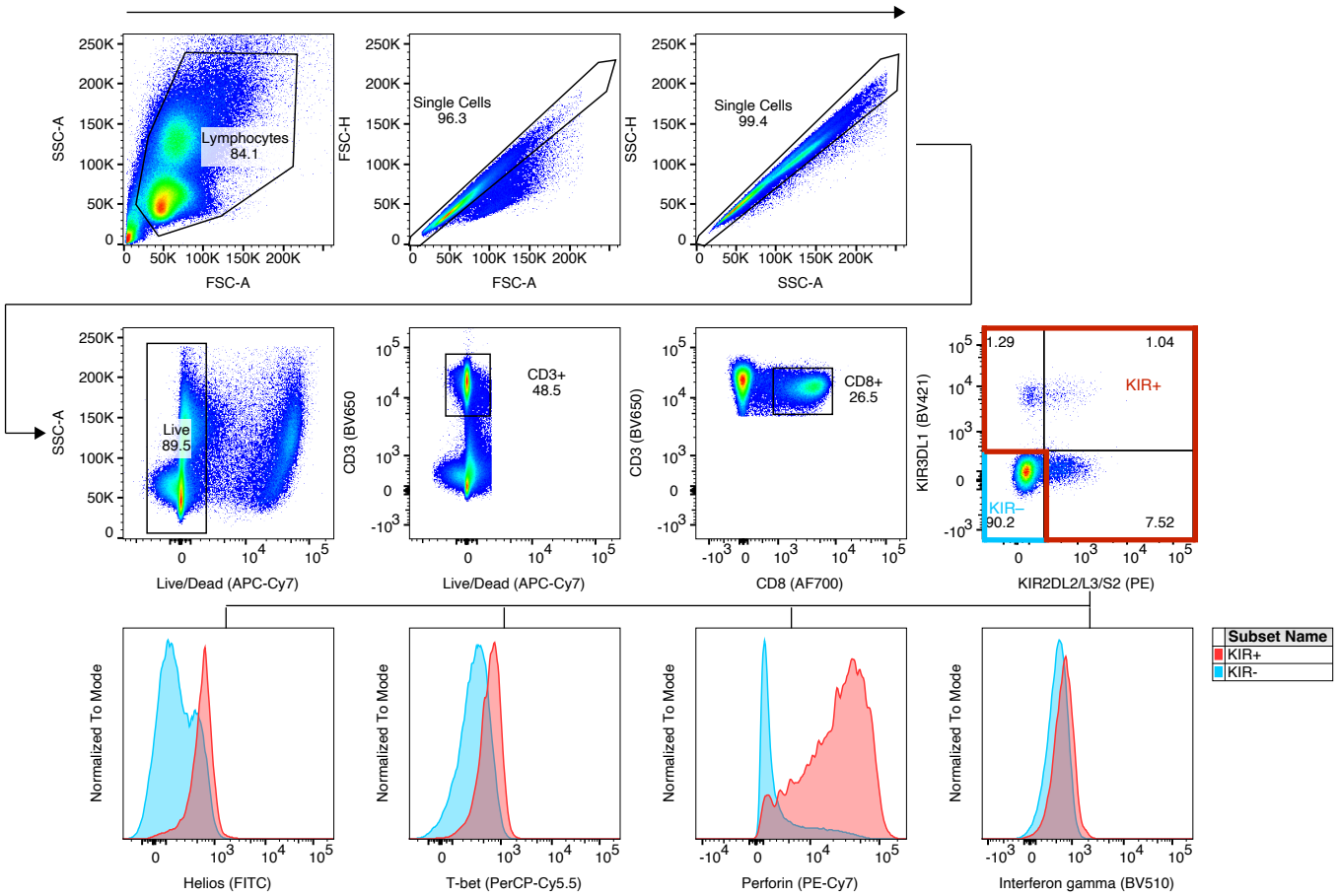

Figure S6: Representative flow cytometry gating strategy for immunophenotyping peripheral blood mononuclear cells. The gating strategy were kept the same across all samples for each experimental batch. Intracellular markers (Helios, T-bet, Perforin, interferon gamma) in KIR^+ (red) and KIR^- (blue) $CD8^+$ T cells in histograms.

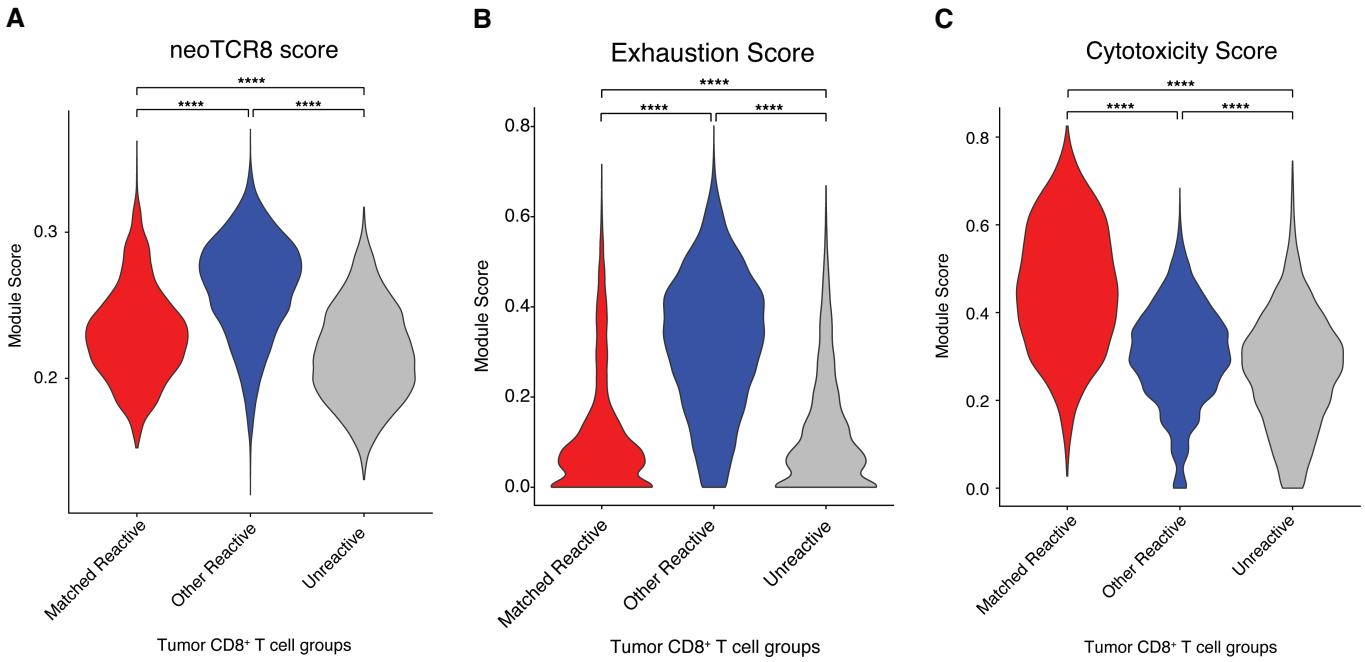

Figure S7: Tumor CD8⁺ T cell gene expression module scores of A) neoTCR8[4], B) Exhaustion[7], or C) Cytotoxicity[7] signatures based on clonal relatedness to blood-based KIR⁺CD8⁺ T cells ("Matched Reactive"), unrelated predicted-reactive ("Other Reactive"), or predicted unreactive T cells ("Unreactive"). Between group differences were determined by Wilcoxon rank sum testing with continuity correction ($p < 0.05$, **** $p < 0.0001$).

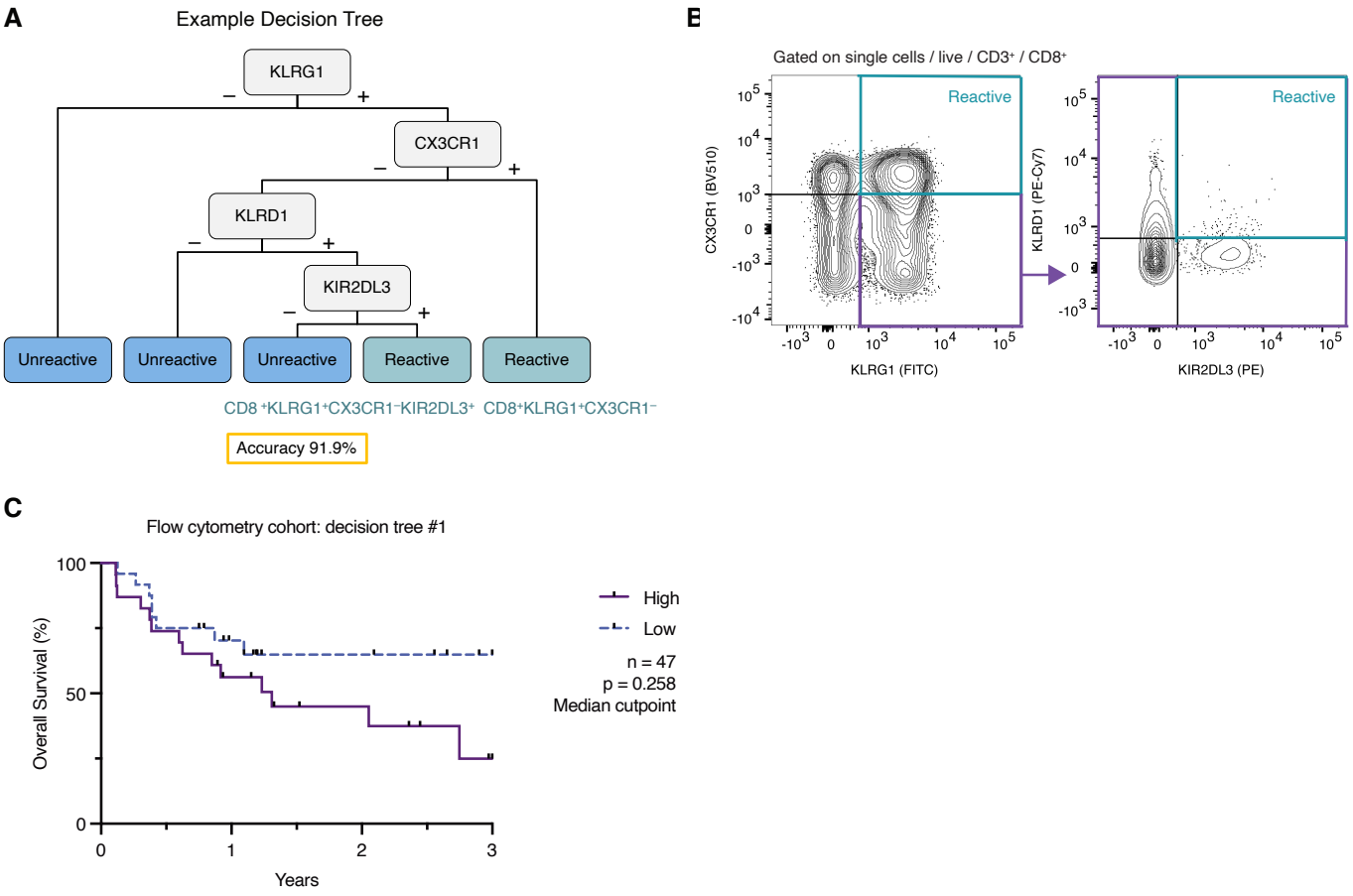

Figure S8: Exploration of surface marker combinations based on Lasso Logistic classifier. A) Decision Tree model to identify combinations of genes identified as predictive of circulating predicted-reactive CD8⁺ T cells by the Lasso Logistic classifier. B) Representative flow cytometry gating of surface marker combinations. C) Kaplan-Meier plots of three-year overall survival based on the high (> median) or low (≤ median) expression of marker combinations. Statistical significance was determined by Gehan-Breslow-Wilcoxon testing ($p < 0.05$).